

Geophysical Effects of the March 29, 2006, Solar Eclipse

Academician of the RAS V. V. Adushkin, B. G. Gavrilov, K. I. Gorelyi,
Yu. S. Rybnov, and V. A. Kharlamov

Received June 14, 2007

DOI: 10.1134/S1028334X07090218

This paper presents results of comprehensive infrasonic, radiophysical, and electromagnetic measurements during the March 29, 2006, solar eclipse. Investigations were carried out in the territory of the Mikhevo geophysical observatory (Institute of Geosphere Dynamics, Russian Academy of Sciences) located 80 km away from Moscow in the Serpukhov area of the Moscow region.

We obtained the following results:

(i) excitation of acoustic-gravitational waves at a frequency close to the Brent–Väsälä frequency ($1.7 \cdot 10^{-3}$ Hz) was recorded in the atmosphere during the maximum phase of the solar eclipse;

(ii) variations were recorded in the total ionospheric electron content (TEC);

(iii) variations in the geomagnetic field, magnetic declination, and inclination were recorded during the maximum phase of the eclipse;

(iv) the spectral density pattern of variations in the near-earth electric field (hereafter, EF) at a frequency of about 10^{-2} Hz coincided in time with variations in the TEC; and

(v) variations were recorded in radiowave propagation along paths intersecting the lunar shadow trajectory.

Geophysical effects accompanying a solar eclipse have always attracted the attention of researchers, because such processes provide insight into the nature and mechanism of perturbations in the Earth's ionosphere and atmosphere related to the influence of the Sun. This issue is discussed in many publications [1–7]. However, comparison of data based on various methods in different geographic zones and heliographic conditions is a difficult task. In this connection, analysis of diverse geophysical data obtained simultaneously at one observation point can undoubtedly provide interesting results.

In the Moscow region, where the measurements were made, the solar eclipse started on March 29, 2006, at 10:10 UT and terminated at 12:18 UT. The maximum phase was recorded at 11:15 UT, and the total duration of the eclipse was ~2 h.

Infrasonic oscillations were recorded by a infralow-frequency microbarometer, which makes it possible to record weak oscillations of atmospheric pressure with an amplitude of $0.1\text{--}10^2$ Pa in the frequency range of $10^{-4}\text{--}20$ Hz. The state of the atmosphere was controlled by a transducer of absolute atmospheric pressure. Figure 1 shows records of infrasonic and atmospheric pressure variations. One can see that the pressure begins to fall virtually with the onset of the eclipse. Based on the frequency analysis, the infrasonic record can be divided into three characteristic periods:

(i) the preeclipse period characterized by background oscillations in the frequency range from $3 \cdot 10^{-4}$ to $5 \cdot 10^{-2}$ Hz related to turbulence of the near-Earth atmosphere (their spectrum corresponds to the relation $f^{-5/3}$);

(ii) the period from the onset of the eclipse to its maximum phase characterized by the disappearance of low frequencies in the range of $(3\text{--}5) \cdot 10^{-4}$ Hz and the appearance of intense infrasonic oscillations in the frequency range of $(1.5\text{--}1.7) \cdot 10^{-3}$ Hz as the maximum phase of the eclipse is approached; and

(iii) the period after the maximum phase of the eclipse characterized by the appearance of oscillations in the frequency range of $(3\text{--}4) \cdot 10^{-4}$ and $(7\text{--}8) \cdot 10^{-4}$ Hz.

Thus, analysis of infrasonic oscillations showed that low-frequency acoustic-gravitational waves, including those in the Brent–Väsälä frequency, are excited as the maximum phase of the solar eclipse is approached and for half an hour after its passage in the atmosphere. Such phenomena are typical of atmospheric fronts and convective thunderstorm cells [8]. Thereby, the maximum effect is shifted to long periods (20–50 min) outward from the lunar shadow.

We also carried out measurements of the TEC with the GPS receiver of the Trimble 5600 type during the solar eclipse. The spectral density pattern of TEC variations (Fig. 2a) shows that strong TEC variations appeared at approximately 07:30 UT, i.e., 2.5 h before

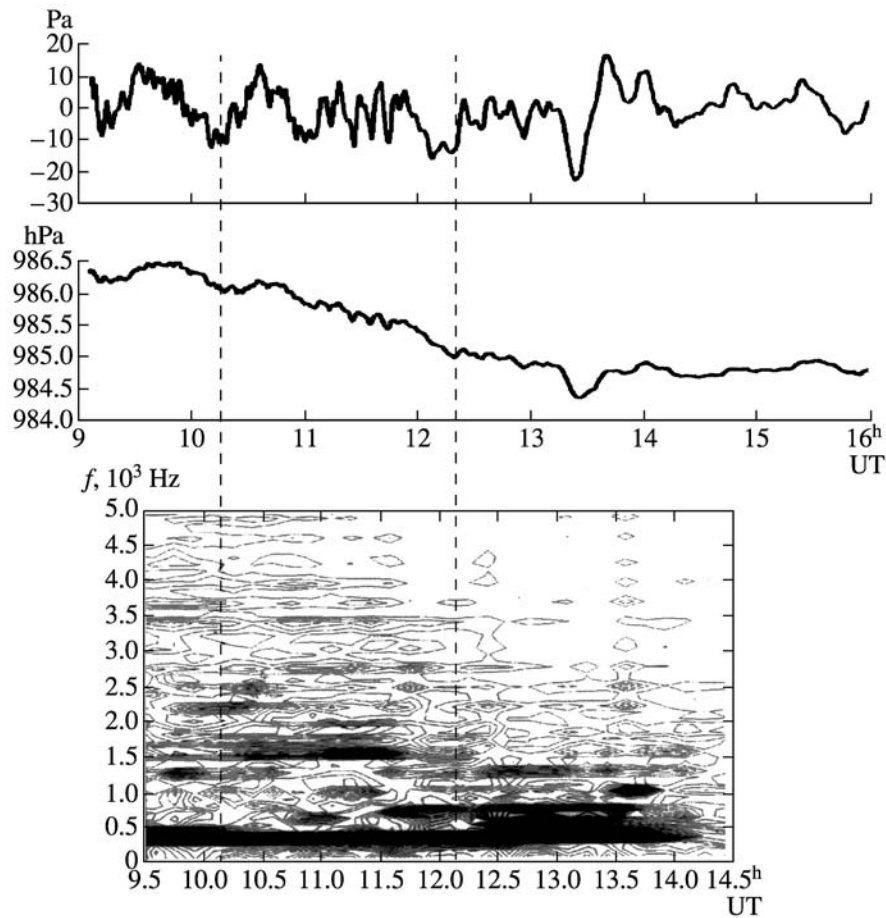


Fig. 1. Variations in infrasound and atmospheric pressure during the solar eclipse and spectrogram of infrasonic oscillations (lower panel). Dashed lines in Figs. 1–3 show the time interval of the eclipse in the observation area.

the onset of the eclipse at the recording point; continued during the entire eclipse period; and terminated at approximately 14:30 UT, i.e., 2 h after termination of the eclipse. Recording of these effects at a distance of more than 2000 km from the zone of complete solar eclipse shows that the ionospheric perturbations were characterized by a global character and rapid distribution over great distances.

The solar eclipse had a significant influence on the parameters of the EF measured by an aerial-type electrometer [9] with a passband of 0–10³ Hz. The record of variations in the TEC voltage during the eclipse (Fig. 2b) shows that the EF voltage rapidly decreased from 320 V/m approximately 0.5 h before the eclipse to 190 V/m at its termination against the background of daily variations. Then, the EF voltage returned to the background value approximately 2 h afterward. The frequency analysis (Fig. 2c) revealed a growth of the spectral density of the EF voltage at a frequency of (0.5–2) · 10⁻⁴ Hz, which coincides in time with the main phase of the eclipse. We should also note the temporal coincidence of these variations with TEC variations.

Geomagnetic effects were investigated using an LEMI 018 vector (three-component) magnetometer. Figure 3 shows the appearance of short-period (~15–20 min) perturbations of the X component of the magnetic field and respective peaks of magnetic declination and inclination recorded at 10:05 and 11:30 UT, i.e., during the main phase of the eclipse. Variations of these parameters can be induced by changes in the configuration of ionospheric current systems related to perturbations in the electron concentration profile and the consequent perturbations in the conductivity of the lower ionosphere due to the change in solar insolation and the generation of wave processes in the ionosphere.

Data on the appearance of such perturbations during the March 29, 2006, solar eclipse are also reported in [7]. The perturbations were recorded near Nizhni Novgorod (frequency reflection method, frequency 2.95 MHz) and Murmansk (vertical sounding method). It was shown that critical ionospheric frequencies f_0E , f_0F1 , and f_0F2 attenuate during the eclipse. Concentrations of electrons were approximately 20 and 15% lower in the E and F1 fields, respectively. At the same time, variations in the ionospheric critical frequency were obviously similar to variations in the horizontal component of

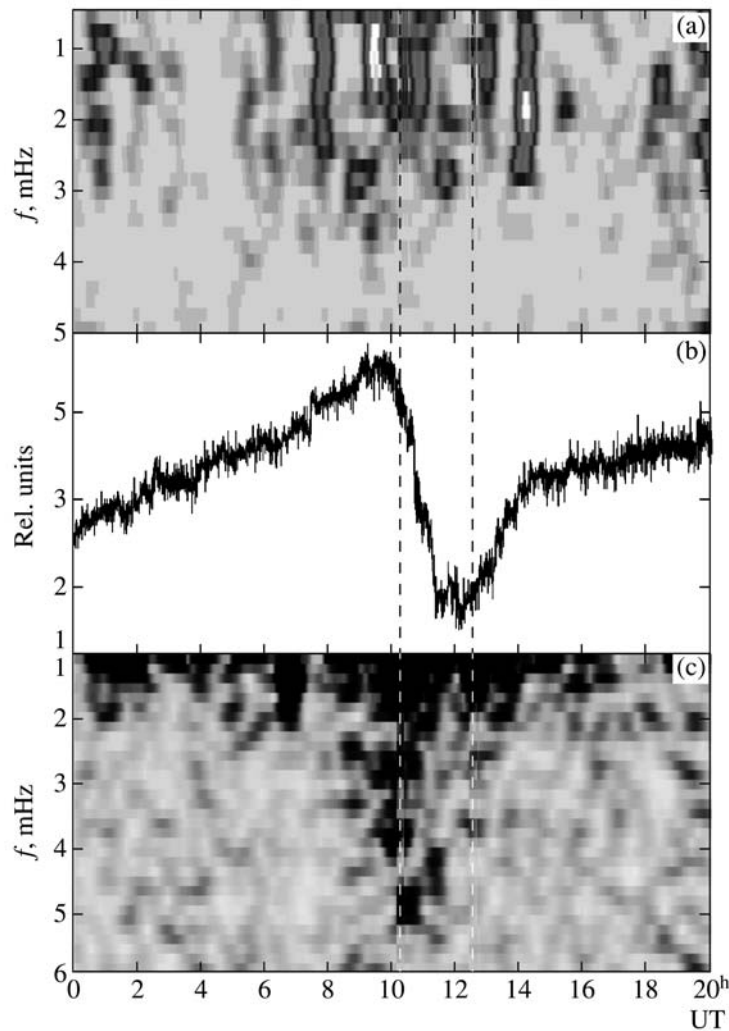


Fig. 2. Spectrogram of variations in the TEC (a), vertical component of the EF (b), and spectrogram of its high-frequency oscillations (c).

the magnetic field at the Mikhnevo observatory (Fig. 3). In addition, the authors of [7] directed attention to quasi-periodic variations in the critical frequency with an oscillation period of 15 min or more. Such oscillations are also typical of variations in the geomagnetic (Fig. 3) and infrasound (Fig. 1) fields during the maximum phase passage. Similar effects were observed during the operation of heating test stands [10].

We observed the effects of the eclipse in the course of recording of the ionospheric state by the tilt sounding method. Radiosignal amplitudes were recorded at the fan of shortwave transmission paths that intersect the trajectory of the total eclipse spot at different angles (Fig. 4). Signals of rotating radiotransmitters located in Israel ($f = 15760$ kHz), Iran ($f = 15150$ kHz), China ($f = 15490$ kHz), and Kuwait were used as reference ones. The state of shortwave transmission paths was investigated by the calibration of radio signals using an IC-R75 scanning shortwave receiver equipped with a pin-type

10-m-high aerial of a circular pattern. Figure 4 (lower panel) presents variations in the radio signal amplitude at three chosen transmission paths that intersect the total eclipse band. One can see that the abrupt onset of attenuation of the signal amplitude (up to the point of their complete disappearance), relative to onset of the total eclipse along the recording paths, is a few minutes ahead of the total eclipse at all observation paths except the Israel–Moscow path, where the attenuation of signals has a lag of 21 min. The duration of the response of transmission paths to the eclipse varies from 20 to 60 min.

The character of the response of transmission paths to the solar eclipse resembles the blackout during solar X-ray bursts (growth of radiowave absorption due to ionization of the ionospheric D region). However, this mechanism is invalid in our case: the solar eclipse rules out the arrival of hard rays to the total eclipse zone. Another mechanism—attenuation of signals due to

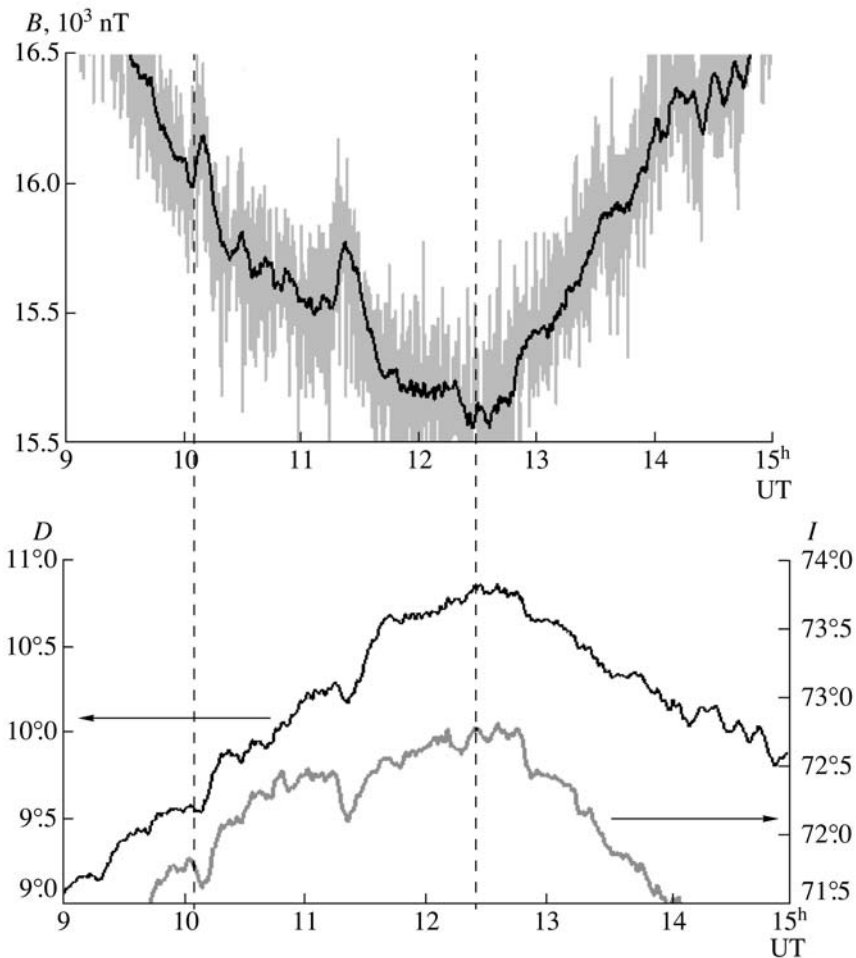


Fig. 3. Variations in the X component of the magnetic field (black curve, 60-s averaging), declination D , and inclination I .

decrease of electron concentration in the F region below the critical frequency level with decreasing ionization of solar radiation—is also hardly possible. Based on data on the vertical sounding in Alma-Ata [6], where the maximum solar eclipse was as much as 76% at 11:48 UT, reduction of the electron concentration at the F2 maximum was no more than 21%. Such a small reduction of the electron concentration cannot provoke the catastrophic attenuation of the signal level at all paths, particularly after the termination of the eclipse. The effects observed during the solar eclipse can be attributed to alternative mechanisms, such as perturbation of the profiles of the ionospheric electron concentration leading to distortion of the shortwave propagation trajectory or generation of global aeronomic processes.

Let us also note that the measurement complex included a system of recording seismic vibrations in the frequency band of 0.5–100 Hz with a sensibility of approximately n nm/s. Processing of seismic signals (frequency and spectral-temporal analysis included) did not reveal any apparent geodynamic effects both

during onset of the solar eclipse and over several hours after its termination.

Thus, the solar eclipse was accompanied by ionospheric perturbations related to both the direct variation of solar radiation and the superposition of perturbations on distribution of the ionospheric electron density above the eastern hemisphere at that time. The superposition of these effects could provoke ionospheric wave perturbations of various types and scales (thermospheric wind, acoustic-gravitational waves, and charged particle precipitation) and the consequent variations in the ionospheric TEC.

Analysis of complex measurements of various geophysical field perturbations provoked by the solar eclipse showed that they are manifested as specific deviations of geophysical fields from the background values. Such deviations can bear important information not only about the energetics and dynamics of their parental processes, but also the characteristics of the environment of their propagation. They can be recorded with the existing devices and scrutinized during the instrumental observations of future solar eclipses.

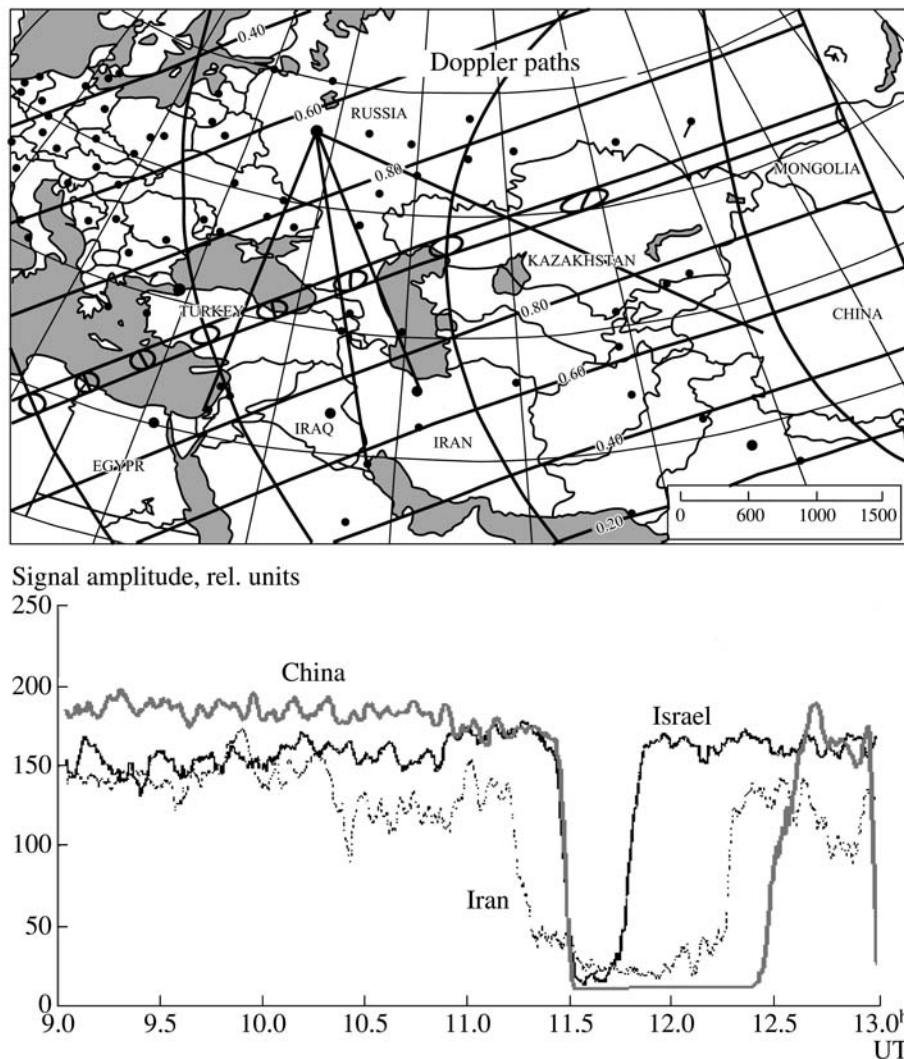


Fig. 4. Schematic transmission paths, movement of the lunar shadow, and variation in the amplitude of radio signals intersecting the shadow trajectory.

ACKNOWLEDGMENTS

This work was supported by the Presidium of the Russian Academy of Sciences (program no. 16), the Earth Sciences Section of the Russian Academy of Sciences (program no. 5), and the Russian Foundation for Basic Research (project no. 07-05-01019).

REFERENCES

1. G. Chimonas and C. O. Hines, *J. Geophys. Res.* **75**, 875 (1970).
2. G. O. Walker, T. Y. Y. Li, Y. W. Wong, et al., *J. Atmos. Terr. Phys.* **53**, 25 (1991).
3. Cheng Kang, Huang Yinn-Nein, and Chen Sen-Wen, *J. Geophys. Res.* **97**, 103 (1992).
4. H. F. Tsai and J. Y. Liu, *J. Geophys. Res.* **104**, 12657 (1999).
5. S. I. Musatenko, O. I. Maksimenko, O. I. Musatenko, et al., *Geomagn. Aeronom.* **46**, 74 (2006) [*Geomagn. Aeronom.* **46**, 78 (2006)].
6. E. L. Afraimovich, S. V. Voeikov, V. V. Vodyannikov, et al., *Ionospheric Effects of the March 29, 2006, Solar Eclipse in Central Asia: Physics of the Near-Earth Space*, in *Proc. BShFF-2006* (2006), pp. 101–103 [in Russian].
7. V. V. Belikov, V. D. Vyakhirev, E. E. Kalinina, et al., Response of Ionosphere to the Partial March 29, 2006, Solar Eclipse Based on Observations in Nizhni Novgorod and Murmansk, in *Proc. XII Conference on the Propagation of Radiowaves* (St. Petersburg, 2006) [in Russian].
8. A. I. Grachev, S. D. Danilov, S. N. Kulichkov, et al., *Izv. Ross. Akad. Nauk, Fiz. Atmos. Okeana.* **30**, 759 (1994).
9. V. I. Baryshev and B. G. Gavrilov, in *Dynamic Processes in Interacting Geospheres* (Geos, Moscow, 2006), pp. 334–340 [in Russian].
10. N. A. Mityakov, V. O. Rapoport, Yu. A. Sazonov, et al., Excitation of Internal Gravitational Waves in the Internal Atmosphere with the Sura Test Bench, Abstracts of Papers, *XIX All-Russia Conference on the Propagation of Radiowaves* (Kazan, 1999) [in Russian].